Proceedings of the IMAC-XXVIII
February 1–4, 2010, Jacksonville, Florida USA

Self-powered Active Control of Structures with TMDs

Xiudong Tang and Lei Zuo

Department of Mechanical Engineering, State University of New York at Stony Brook

Stony Brook, New York 11794

Email: lei.zuo@stonybrook.edu

NOMENCLATURE

M, K, C	Mass, stiffness and damping matrices
k_t,k_e	Thrust constant and back electromotive force coefficient of electromagnetic motor
R, L, C	Electrical resistance, inductance and capacitance
C_d	The object's drag coefficient,
f, μ	Turning ratio, mass ratio of TMD
ξ	Damping ratio
F, u	Excitation and control forces
x_s, x_1	Displacements of structure and TMD

ABSTRACT

This paper studies the feasibility of self-powered active vibration control of structures with Tuned Mass Dampers (TMDs). Without consuming external energy, the proposed self-powered vibration control strategy can provide better performance than the passive TMD in mitigating the vibration of buildings induced by wind load. The vibration-dissipative element of TMD is replaced with an electromagnetic machine, which serves as actuator and harvester at the same time. First, the desired force is obtained by adopting Linear Quadratic Regulator (LQG) optimal control. Then, the self-powered active control strategy is designed based on the essence of the desired force, which can be passive or active types. The energy of the vibration can be harvested as electricity in *energy harvesting mode*, and pumped back into the mechanical system when instant active force is required. Switch based circuits with capability of bi-directional power flow are presented for the implementation of self-powered active TMDs. With taking the efficiency of the harvesting and driving circuits into account, numerical simulations are carried out based on a tall building with a TMD under random and harmonic excitations. The results indicate the feasibility and effectiveness of self-powered active TMDs.

1. INTRODUCTION

Vibration has been a serious concern since the early days when the tall buildings or long-span bridges were built. These structures are subjected to huge dynamic loadings from the winds, earthquakes, water waves, traffics, and human motions. The large vibration amplitude can damage the structures or the secondary components, or cause discomfort to its human occupants [1]. Extensive research has been conducted to mitigate this harmful vibration, by, for example, structure design [2], vibration isolation systems [3], and auxiliary damping systems. Among these methods, the TMD has been proved to be a very simple and effective vibration suppression device, with many

practical implementations on tall buildings, such as Taipei 101 in Taipei, Citi Group in New York, and many others. The original TMD, which was invented by Frahm in 1911 [4], only consists of an auxiliary mass and a spring connected to the primary system to mitigate vibration in a very narrow frequency range near the resonance. Ormondroyd and Den Hartog [5] increased the working frequency range by introducing an additional damper.

Although TMD composes the greatest percentage of the supplemental damping systems currently in use, it has its inherent drawbacks. When the parameters of the primary systems change a small amount, the performance of TMDs will be greatly defected. It is so called off-tuning problem, which has been investigated by researchers, for example, Bergman [6] and Setareh [7]. Hence, active TMD is developed to handle this problem. It has been proved that the active TMD can provide better vibration mitigation performance than the passive one, at the cost of large amount energy [8]. However, the active TMD system is more complex and costly, which limits its practical implementations. Particularly active TMDs suffer from the inherent disadvantage that it relies on external energy, which is not countable in the hazardous situations like earthquakes or hurricanes. Hybrid active TMD, which is composed of passive TMD and one additional actuator, can reduce the power consumption and increase the robustness in the event of power failure [9, 10].

Realizing both the vibration mitigation performance as well as the limitations of active TMDs, researchers proposed semi-active TMDs to provide better vibration mitigation performance than the passive one without the drawbacks of active TMDs. Semi-active control using Magneto Rheological (MR) or variable orifice dampers has been investigated by many researchers [11-15], especially in vibration control of buildings with TMDs [14] and vehicle suspension systems [15].

In this paper, we proposed a self-powered active vibration control of TMD, which can provide better vibration mitigation performance than the passive TMD, without consuming external energy. The auxiliary damper of classic TMD is replaced with an electromagnetic motor, which acts both actuator and harvester in this self-powered active TMD. The kinetic energy of vibration is harvested and stored, and then used when instant active force is required. At first, the feasibility of self-powered active vibration control is studied. We classify the desired force obtained by LQG optimal control design into two categories: passive force and active force, resulting two working modes of self-powered active TMD, named as energy harvesting mode and driving mode. A switch based circuit is proposed to realize the bi-directional power flow control. With taking the efficiency and parasitic power of the circuit into account, numerical simulations are carried out based on a tall building with TMD. The results under random and harmonic excitation show that the self-powered active TMD more effective than the passive one in mitigating the vibration.

This paper is organized as follows: In Section 2, the feasibility of self-powered active vibration control of TMD will be conducted, using LQG optimal control methods. The realization of self-powered active TMD is introduced in Section 3, where the circuit capable of bi-direction power flow is also discussed. In Section 4, the extensive numerical study will be carried out, where the vibration performances of building structures with passive and active TMDs are compared and the energy balance is also analyzed with taking the efficiency and parasitic power into account. Then conclusions follow as Section 5.

2. FEASIBILITY STUDY OF SELF-POWERED ACTIVE TMD

Figure 2.1 shows the modeling of building with TMD, where the building is considered as single degree-of-freedom (SDOF) system and the damper of the TMD is replaced with an electromagnetic motor. The primary structure is subjected to the wind load disturbance F. The force u is exerted by the electromagnetic motor. Then, the dynamics equations of this building with TMD can be written as:

$$\begin{cases} m_s\ddot{x}_s + k_s x_s + c_s\dot{x}_s = k_1(x_1 - x_s) + F - u \\ m_1\ddot{x}_1 + k_1(x_1 - x_s) = u \end{cases} \tag{1}$$

which can be further expressed in the following form:

$$\mathbf{M}\ddot{\mathbf{x}}(t) + \mathbf{K}\mathbf{x}(t) + \mathbf{C}\dot{\mathbf{x}}(t) = \mathbf{G}F(t) + \mathbf{H}u(t) \tag{2}$$

where $\mathbf{M} = \begin{bmatrix} m_s & 0 \\ 0 & m_1 \end{bmatrix}$, $\mathbf{K} = \begin{bmatrix} k_s + k_1 & -k_1 \\ -k_1 & k_1 \end{bmatrix}$, $\mathbf{C} = \begin{bmatrix} c_s & 0 \\ 0 & 0 \end{bmatrix}$, $\mathbf{G} = \begin{bmatrix} 1 \\ 0 \end{bmatrix}$, $\mathbf{H} = \begin{bmatrix} -1 \\ 1 \end{bmatrix}$, $\mathbf{x}(t) = [x_s \;\; x_1]^T$

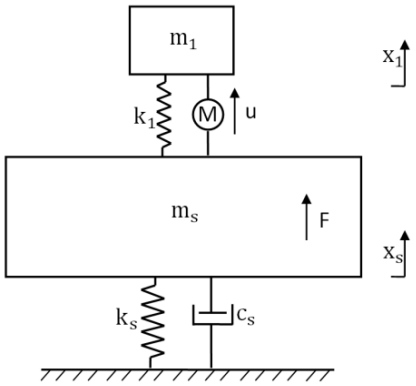

Figure 2.1 - Modeling of Building with TMD

Defining the state space as $\mathbf{q} = [q_1, q_2, q_3, q_4]^T = [x_s, x_1, \dot{x}_s, \dot{x}_1]^T$, (2) can be further written in the state space form:

$$\dot{\mathbf{q}}(t) = \mathbf{A}\mathbf{q}(t) + \mathbf{B_f}F(t) + \mathbf{B_u}u(t) \tag{3}$$

where $\mathbf{A} = \begin{bmatrix} \mathbf{0} & \mathbf{I} \\ -\mathbf{M^{-1}K} & -\mathbf{M^{-1}C} \end{bmatrix}$, $\mathbf{B_f} = \begin{bmatrix} \mathbf{0} \\ \mathbf{M^{-1}G} \end{bmatrix}$, $\mathbf{B_u} = \begin{bmatrix} \mathbf{0} \\ \mathbf{M^{-1}H} \end{bmatrix}$.

Tall buildings are usually subjected to tremendous wind load disturbance, which accounts as the main reason for the overall vibration of the building, since the local load is governed by the seismic stress and the overall motion is governed by the wind load [16]. The amplitude of dynamic wind load on the structures can be calculated as [17]:

$$F = \frac{1}{2}\rho A V^2 C_d \tag{4}$$

where ρ is the air density, V is the wind speed, and A is the projected area of the building perpendicular to the wind velocity, C_d is the object's drag coefficient, which depends on the shape of the object (about 1 for a cylinder). The wind force is usually very large, for example, using (4), the dynamic load of breeze at the speed of 12 MPH on a high-rise building of 1440ft (Taipei101) height and slenderness (height to width) ratio 9 is estimated to be 400kN, or 40 tons. Besides, the frequencies of wind load vary in a range, which can be modeled as Gaussian white noise with certain power density. Hence, it is more suitable to use LQG control as the optimal control strategy. The feedback measurements we choose are the accelerations of the main structure and auxiliary mass.

First, the desired active force u_{des} is obtained by LQG active controller design. Then u_{des} is clipped into two categories: passive force and active force. Then the self-powered active control strategy is design to make the actual force follow the desired force as much as possible. To get the desired force, the root-mean-square (RMS) value is used as the performance index to evaluate the output performance, where the output is the acceleration of the primary system, expressed as:

$$z(t) = \mathbf{C_2}\mathbf{q}(t) + \mathbf{D_{22}}\mathbf{F} \tag{5}$$

where $\mathbf{C_2} = \left[-\left(\frac{k_s}{m_s} + \frac{k_1}{m_s}\right), \frac{k_1}{m_s}, -\frac{c_s}{m_s}, 0\right]$, $\mathbf{D_{22}} = [1/m_s]$.

Hence the performance index in chosen to minimize the RMS acceleration of the building under limited control effort:

$$J = \int_0^\infty (z^2 + ru^2)\, dt = \int_0^\infty \begin{bmatrix} \mathbf{q} \\ u \end{bmatrix}' \mathbf{T} \begin{bmatrix} \mathbf{q} \\ u \end{bmatrix} dt \tag{6}$$

where **T** is obtained as:

$$\mathbf{T} = \begin{bmatrix} \mathbf{C_2}'\mathbf{C_2} & \mathbf{C_2}'\mathbf{D_{22}} \\ \mathbf{D_{22}}'\mathbf{C_2} & \mathbf{D_{22}}'\mathbf{D_{22}} + \mathrm{r} \end{bmatrix} \tag{7}$$

By minimizing the quadratic cost, we can minimize the response to Gaussian white noise input. Denoting $\mathbf{Q} = \mathbf{C_2}'\mathbf{C_2}, \mathbf{N} = \mathbf{C_2}'\mathbf{C_2}, \mathrm{R} = \mathbf{D_{22}}'\mathbf{D_{22}} + \mathrm{r}$, the optimal control law is expressed:

$$\mathrm{u_{des}} = -\mathrm{R}^{-1}(\mathbf{B_u^T S} + \mathbf{N^T})\mathbf{q}(t) = -\mathbf{K}\mathbf{q}(t) \tag{8}$$

where **S** is the solution of the algebraic Riccati Equation (ARE):

$$\mathbf{A^T S} + \mathbf{S A} - (\mathbf{S B_u} + \mathbf{N})\mathrm{R}^{-1}(\mathbf{B_u^T S} + \mathbf{N^T}) + \mathbf{Q} = 0 \tag{9}$$

Since we use acceleration feedback, not all the states are available as feedback. LQG state-estimator is employed to estimate the state vector q(*t*) in (3). The feedback measurement $\mathbf{y}(t)$ can be expressed in the form of

$$\mathbf{y}(t) = \mathbf{C_1 q}(t) + \mathbf{D_{12} F} + \mathbf{D_{11} u} \tag{10}$$

This LQG state-estimator is so called Kalman filter, the equation of which can be expressed as:

$$\dot{\tilde{\mathbf{q}}}_{(t)} = \mathbf{A}\tilde{\mathbf{q}}_{(t)} + \mathbf{B_u}\mathrm{u_{des}} + \mathbf{L}\left(\mathbf{y}_{(t)} - \mathbf{C_1}\tilde{\mathbf{q}}_{(t)} - \mathbf{D_{12}}\mathrm{u_{des}}\right) \tag{11}$$

where $\tilde{\mathbf{q}}_{(t)}$ is the estimated state vector. The observer gain matrix **L** is obtained as:

$$\mathbf{L} = \mathbf{P C_1^T V^{-1}} \tag{12}$$

where **V** is the covariance matrix of the measurement noise, and **P** is the solution of ARE:

$$\mathbf{A P} + \mathbf{P A^T} - \mathbf{P C_1^T V^{-1} C_1 P} = 0 \tag{13}$$

In order to verify the feasibility of self-powered active vibration control, the numerical simulation using the active controller design described above is carried out based on Taipei101, one of the tallest buildings in the world. It is installed with TMD of 730 tons (mass ratio μ=0.78%), where μ is ratio of total auxiliary masses over the modal mass of the primary system, which is typically 1/3 of the building mass [16]. The parameters of the stiffness and damping coefficient of the passive TMD are optimized using the method in the paper by Warburton [18], where the tuning ratio f_1 and damping ratio ζ_1 are given by:

$$f_1 = \frac{1}{(1+\mu)^{1/2}} \tag{14}$$

$$\zeta_1 = \sqrt{\frac{3\mu}{8(1+\mu/2)^3}} \tag{15}$$

For the active TMD, the tuning ratio is the same as the passive one. However the damper is replaced with an electromagnetic motor. The active TMD is obtained using the LQG control design described above, when subjected to a wind load disturbance with the power spectral density of S_0=4·10^{14}N^{2}s. Without considering practical implementation, the power is estimated by multiplying the desired force and relative velocity between the auxiliary mass and primary structure.

$$P = u_{des} \cdot v_r \tag{16}$$

Figure 2.2 shows the transient response of energy and power using active control, when the building is subjected to random wind load disturbance. It can be seen from the figure that the power on the transducer may be positive or negative, which means the power flow is bi-directional. From the total energy goes through the transducer, we can see that it is negative after 40 seconds, which means the system is still dissipating energy. Ideally, more energy can be harvested than that used for active force. It should be noted that Nakano and Suda [19] investigated self-powered active control of vehicle suspension using sky-hook control and Scruggs [20] also

investigated the feasibility based on PID control law. From figure 2.2, we can also conclude that there is minimum value of the capacity of the external reservoir. At the beginning, active force is required more frequently. As time goes by, the external reservoir is charged and the energy can be further used for active control. Without the initial energy reservoir, the system will be uncontrolled at the beginning, however, after a while the reservoir will be charged and the system can work continuously. And the excessive harvested energy can be used for other purposes, for example, to power the utilities or feed the electricity grid.

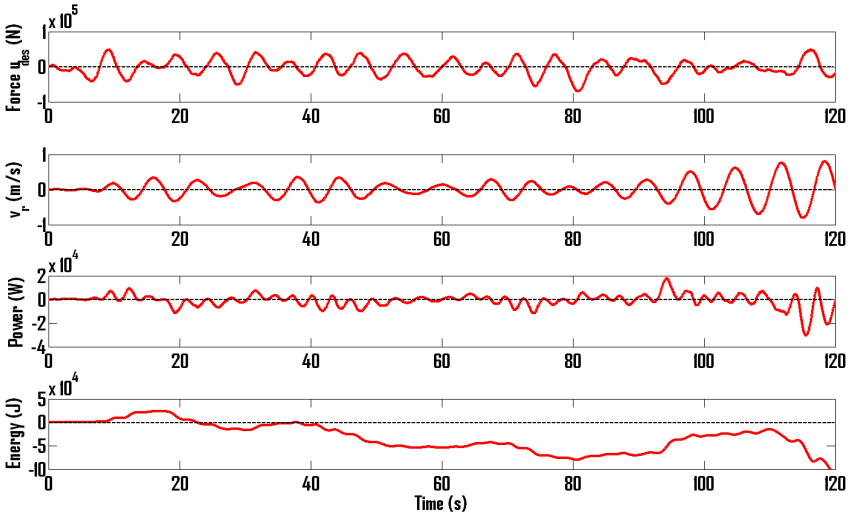

Figure 2.2 - Transient response of force, velocity, energy and power active TMD under random excitation

3. DESIGN OF THE SELF-POWERED ACTIVE TMD

In section 2, we discussed the feasibility of self-powered active vibration control of TMD, and found that even the pure active controlled TMD is essentially dissipative, which means system is still dissipating energy. In this section, we are discussing the realization of self-powered active TMD, including the control strategy of the switches based circuit, which is capable of bi-directional power flow.

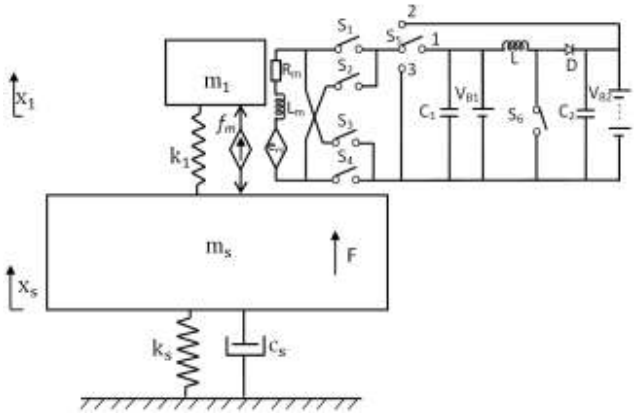

Figure 3.1 - Schematic of the self-powered active TMD system

Figure 3.1 shows the schematic of the self-powered active TMD, with the mechanical system coupled with electric circuit, which is controlled by the switches S_1-S_6. The electromagnetic motor is modeling as a voltage source with the inherent conductor L_m and resistor R_m connected in series. The relative motion between the two masses can induce a voltage e_m in the coils, which is proportional to the relative velocity of stator and rotor $v_r = \dot{x}_1 - \dot{x}_s$. Magnification mechanisms may exist, therefore, the relative speed between the stator and mover can be *M* times the relative motion between the TMD and the structure.

$$e_m = Mk_e v_r \tag{17}$$

where k_e is the back electromotive force coefficient (EMF) of the electromagnetic motor. Meanwhile, the current flows inside of the motor coil will induce a back electromotive force proportional to the current:

$$f_b = Mk_t i \tag{18}$$

where k_t is thrust constant of electromagnetic motor.

The energy is harvested and first stored in battery B1 with low voltage level and then the voltage is further boosted to charge the battery B2 with high voltage level, which is used to drive the motor when active force is required. The self-powered active TMD works in three different modes: (1). energy harvesting mode. When the desired force has the opposite direction of the relative velocity between the two masses, the desired force is essentially a passive force. In this mode, the electromagnetic motor works in driven mode, acting as energy harvester and the switch S_5 is switched to contact 1. (2). driving mode. When the desired force has the same direction as the relative velocity, the desired force should be realized by active force. The electromagnetic motor works as actuator and S_5 is switched to contact 2. (3). passive mode. The voltage generated by the electromagnetic motor maybe not large enough to overcome the battery voltage V_{B1}. The electromagnetic motor is set to be closed-circuit by switching S_5 to contact 3. In these three modes, the control schemes of the switches S_1-S_6 are different.

3.1. ENERGY HARVESTING MODE

When the desired force and the relative velocity have the opposite direction and the voltage generated by the electromagnetic mode is larger than the voltage of the first battery V_{B1}, the system will work in energy harvesting mode. In this mode, S_5 is switched to contact 1. Energy is harvested and stored in battery B_1 and booster DC-DC converter is used to step-up the voltage to further charge the battery B_2 which has high voltage.

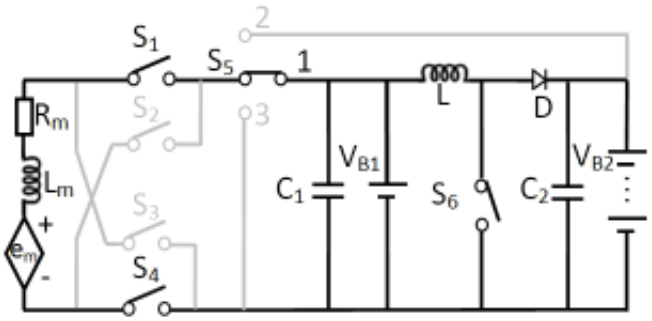

Figure 3.2 - Energy harvesting mode (e_m>0)

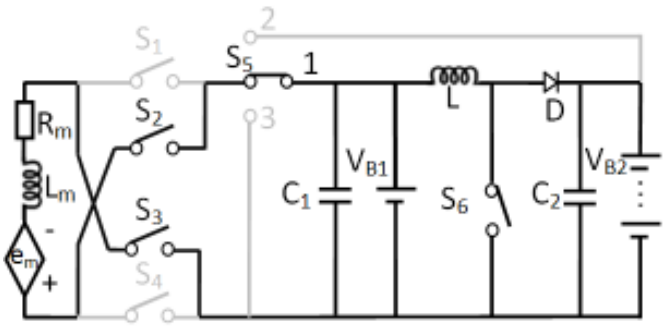

Figure 3.3 - Energy harvesting mode (e_m<0)

Figure 3.2 and figure 3.3 show the circuit in this mode. Either switch pair S_1 and S_4, or S_2 and S_3 is involved, since the direction of the relative velocity varies. In this way, the two switch pairs serve as synchronous rectifier. The corresponding passive force can be expressed as follows, when the inductance L_m is negligible:

$$f_m = -sign(v_r)\frac{Mk_t(Mk_e|v_r|-V_{B1})}{R_m} \tag{19}$$

where sign() is the signum function. In energy harvesting mode the passive force is composed of a viscous damping component $-M^2k_tk_ev_r/R_m$ and a force $sign(v_r)V_{B1}/R_m$ due to the battery B_1. Vibration mitigation performance can be further improved, if the actual force can be controlled to follow the desired force, by applying Pulse-Width Modulation (PWM) to the switch pairs. Hence, the force provided by the electromagnetic motor can be controlled by adjusting the duty cycle of the switch pair S_1 and S_4, or S_2 and S_3. The work principle is similar to the switching amplifier. Hence the force can be expressed as:

$$f_m = -sign(v_r)\frac{Mk_t(DMk_e|v_r|-V_{B1})}{R_m} \tag{20}$$

The duty cycle corresponding to the desired force u_{des} can be expressed as:

$$D = \frac{|u_{des}|R_m}{M^2k_ek_t|v_r|} + \frac{V_{B1}}{Mk_t} \tag{21}$$

The passive damping force can be provided in this mode is limited due to the fact that D should be smaller than one. The damping force is set to be maximum (D=1) when it is out of the limitation:

$$f_{mmax} = -sign(v_r)\frac{Mk_t(Mk_e|v_r|-V_{B1})}{R_m} \tag{22}$$

3.2. DRIVING MODE

When the desired force and the relative velocity have the same direction, the self-powered active TMD will work in driving mode, where the electromagnetic motor acts as actuator. The circuit involved in this mode is actually classic D amplifier [21], where the direction and amplitude of the voltage applied on the electromagnetic motor can be controlled.

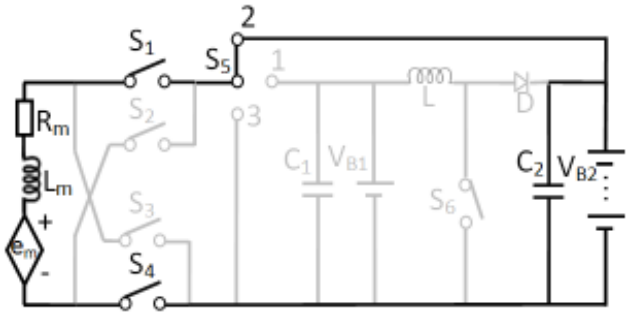

Figure 3.4 – Driving mode (f_m>0)

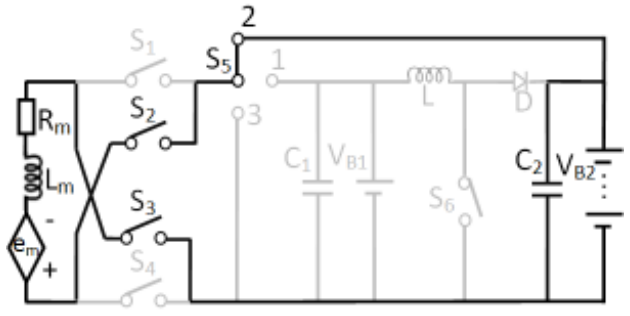

Figure 3.5 – Driving mode (f_m<0)

As shown in figure 3.4 and figure 3.5, the direction of the voltage is controlled by switching the two pairs of switches. The voltage amplitude is controlled by the duty cycle of the PWM applied on the switch pair. The circuit is classic D amplifier, the output voltage of which is proportional to the duty cycle. Hence, the output active force of the electromagnetic motor is:

$$f_m = \frac{Mk_t(DV_{B2} - Mk_e|v_r|)}{R_m} \tag{23}$$

The duty cycle provided by the controller in order to follow the corresponding desired force u_{des} can be expressed as:

$$D = \frac{|u_{des}|R_m}{Mk_tV_{B2}} + \frac{Mk_e|v_r|}{V_{B2}} \tag{24}$$

3.3. PASSIVE MODE

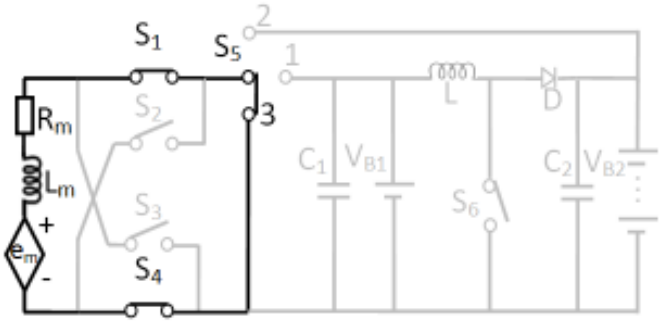

Figure 3.6 - Passive mode

When the desired force and the relative velocity have the opposite direction, however, the voltage generated by the electromagnetic motor is not large enough to overcome the voltage of the first battery V_{B1}, the system will work in this mode. In this mode, the switch S_1 and S_4 is switched on and S_5 is switched to contact 3. In the passive mode, the electromotive force will appear to be an ideal viscous damping force:

$$f_m = \frac{M^2k_tk_ev_r}{R_m} \tag{25}$$

4. NUMERICAL SIMULATIONS

The simulations are carried out based on the building Taipei 101. The parameters of Taipei 101 have been described in section 2 (m_1=730 tons, mass ratio μ=0.78%). And the damping ratio of the primary system is assumed to be 1% [22]. For the electromagnetic motor, the thrust constant k_t, Back-EMF constant k_e and the resistance R_m are the inherent parameters of the electromagnetic motor. From the specification data of commercialized *IC44 series* linear electromagnetic motors manufactured by *Kollmorgen* [23], k_t ranges from 72.7N/A to 1210 N/A, k_e ranges from 59.3V·s/m to 988 V·s/m, R_m ranges from 0.37Ω to 38.6Ω. Hence, in this simulation k_t and k_e are chosen to be 700N/A and 700V·s/m. R_m is 20 Ω and the motion magnification mechanism M is set to be 2. Figure 4.1 compares the transient response of the structure's acceleration when subjected to the random wind disturbance with the power spectral density of S_0=4.0x10^{14} N^2s. And the RMS of the output for structures with different TMDs is shown in Table 4.1.

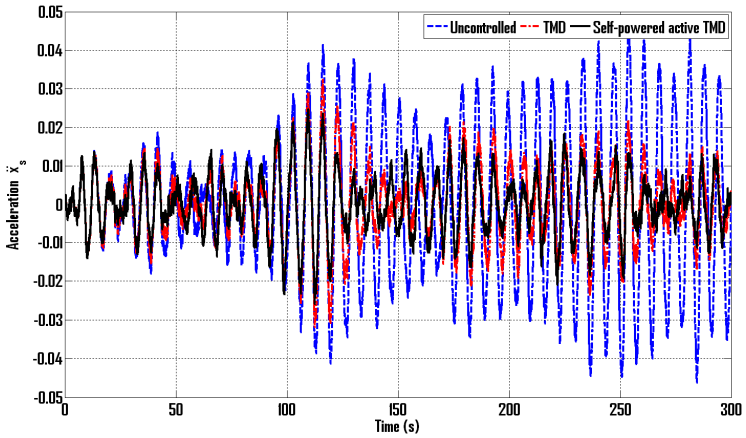

Figure 4.1- Transient acceleration response under random excitation

Table 4.1 – RMS acceleration of the building under random wind load excitation with the power spectral density of $S_0=4.0\times10^{14}$ N^2s

TMD type	RMS of the acceleration (m/s^2)
Uncontrolled	0.018903
TMD	0.008267
Active TMD	0.006805
Self-powered active TMD	0.007345

Figure 4.2 shows the transient force response of self-powered TMD and the active TMD. As we can seen from the figure, there are three types of forces expressed by (20), (23), (25), corresponding to the threes working modes: harvesting, driving, and passive.

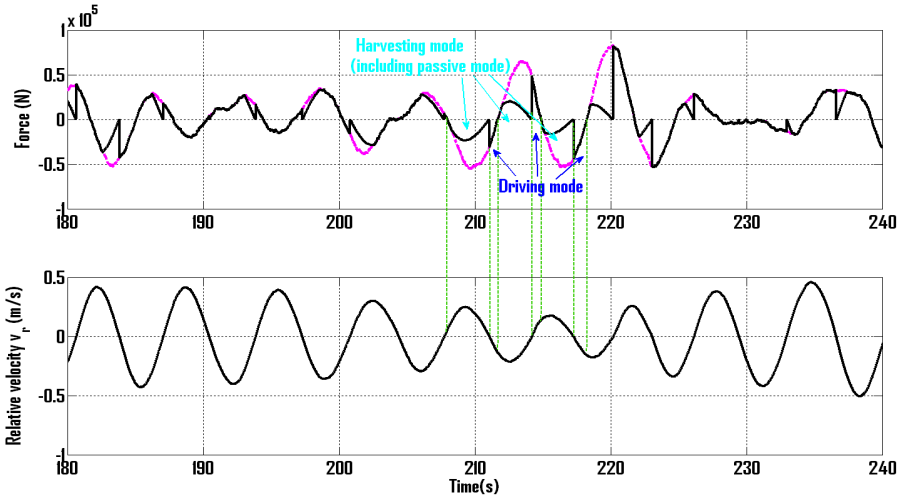

Figure 4.2- Transient force response under random excitation. (Passive mode is a small segment marked in the harvesting mode in this figure when the relative velocity $|v_r|$ is less than Mk_eV_{B1}/R_m.)

Because of the nonlinearity of self-powered active control law, the system is no longer linear. However, we find that the excitation amplitude has little effect on the frequency response of transmissibility ratio, when the wind load disturbance is large. Figure 4.3 shows the transient response of the primary system subjected to harmonic excitation with a frequency of 0.146 Hz (natural frequency of the building) and amplitude of 250kN. As seen from Figure 4.3, the transient response of the self-powered active TMD can go into steady state after a few periods. This figure also indicates that at this frequency the self-powered active TMDs can reduce the vibration to 56.6% over the passive TMD. For this reason, we compare the frequency responses of transmissibility ratios of different TMDs. Figure 4.4 shows the frequency response of the self-powered TMD, compared with the passive and active TMD.

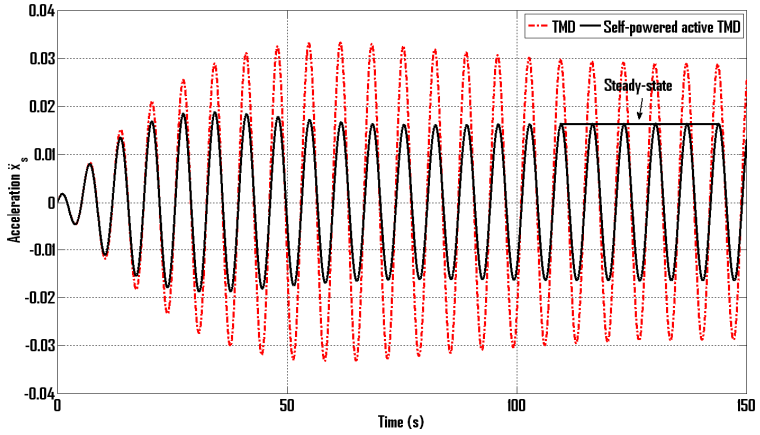

Figure 4.3 – Transient response under harmonic excitation

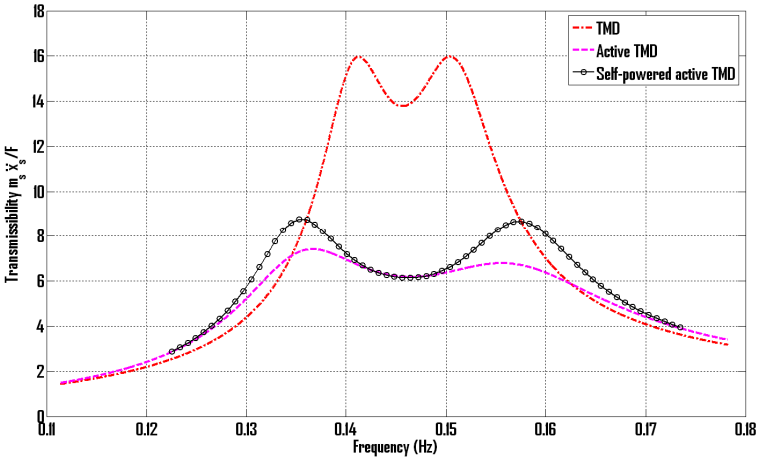

Figure 4.4 Frequency responses of transmissibility ratio $m_s\ddot{x}_s$ /F.

As discussed in section 3, the circuit is actually classic D amplifier in driving mode. The classic D amplifier has very high power conversion efficiency, usually>90% [24]. In the energy harvesting mode, the booster DC-DC converter has a typical efficiency of 78%, accounting for the main power loss. With taking both the self-powered active control law and parasitic power loss into account, we plotted the instant power and accumulated energy of the system in figure 4.5. shows that the self-powered active control is still feasible when subjected to random disturbance with the power spectral density of S_0=4.0x10^{14}N^{2}s. The system can harvest more energy than needed for the active control part.

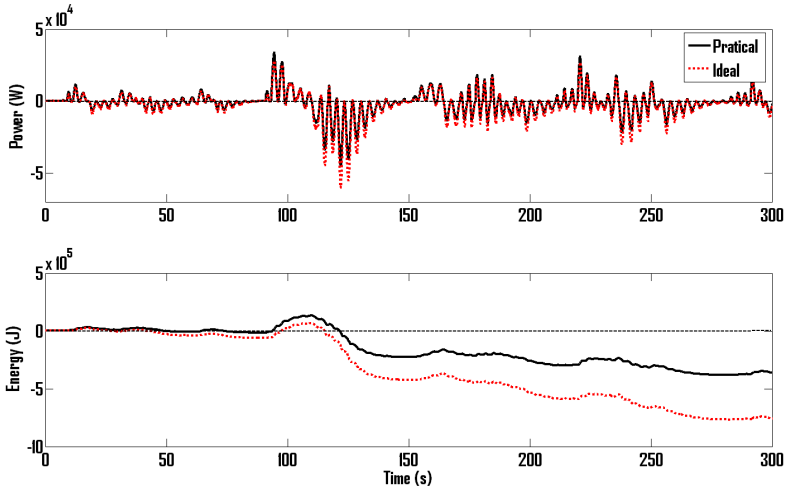

Figure 4.5 Power and energy transient response. The ideal case is the one doesn't consider the any power loss, while the practical take the efficiency of both harvesting and driving circuit into account.

5. CONCULSION

This paper investigated the feasibility and realization of self-powered active control of TMD. Without consuming external energy, the proposed self-powered active TMD can provide better vibration mitigation performance compared with the passive TMD. Switch based circuits with capability of bi-directional power flow are presented for the implementation of self-powered active TMD. The power balance is analyzed with taking the efficiency of circuit and parasitic power loss into account. It also should be noted that a pre-charged energy reservoir may be used to jump-start the system before the system maintains the performance itself, but this pre-charged energy reservoir is not necessary.

6. REFERENCE

[1] Kareem, A., Kijewski, T. and Tamura, Y., "Mitigation of Motions of Tall Buildings with Specific Examples of Recent Applications," *Wind and Structures*, Vol 2, n3, pp 201-251, 1999.

[2] Ali, M.M. and Moon K.S., "Structural Developments in Tall Buildings: Current Trends and Future Prospects", *Architectural Science Review*, Volu 50 n3, pp 205-223, 2007

[3] Morgan,T.A and Mahin, S.A., "Development of a Design Methodology for Seismic Isolated Buildings Considering a Range of Performance Objectives", *Proceedings, 4th International Conference on Earthquake Engineering, NCREE*, Taipei, Taiwan, 2006

[4] Frahm, H., "Device for Damping Vibrations of Bodies," *U.S. Patent No.989, 958*, 1911.

[5] Den Hartog, J. P., *Mechanical Vibration*, McGraw-Hill, New York, 1947.

[6] Kerschen, G., Kowtko, J. J., McFarland, D. M., Bergman, L. A. and Vakakis, A. F., "Theoretical and experimental study of multimodal targeted energy transfer in a system of coupled oscillators", *Nonlinear Dynamics*, vol. 47, pp. 285.309, 2007.

[7] Setareh, M., Ritchey, J.K., Baxter, A.J. and Murray, T.M., "Pendulum tuned mass dampers for floor vibration control". *J Perf Constr Fac* 20(1): 64–73, 2006

[8] Koshika, N., Sakamoto, M., Sasaki, K., Ikeda, Y. and Kobori, T., "Control effect of active mass driver system during earthquakes and winds", *Proc 1st MOVIC Conf, Yokohama*, Japan, 1992, pp 261-266

[9] Fujino, Y., Soong, T.T. and Spencer, B. F., "Structural Control: Basic Concepts and Applications", *the Proceedings of the 1996 ASCE Structures Congress,* 1996

[10] Tomoo, S. and S. Keiji. (1998), Dynamic Characteristics of a Triangular-Plan High-Rise Building and Its Active Vibration Control System, Proceedings of Structural Engineers World Congress, San Francisco, CD-ROM: T198-5.

[11] Pinkaew, T. and Fujino, Y., "Effectiveness of semi-active tuned mass dampers under harmonic excitation", *Engineering Structures*, Volume 23, Issue 7, pp. 850-856, July 2001.

[12] Dyke, S. J., Spencer, B. F, Sain, M. K. and Carlson, J. D., "Modeling and control of magnetorheological dampers for seismic response reduction", *Smart Mater. Struct*. 5 pp. 565-575,1996.

[13] Lewandowski, R. and Grazymislawska, J., "Dynamic behavior of composite mass damper for control of wind-excited vibration", *AMAS Workshop on Smart Materials and Structures*. pp.131–140 Jadwisin, September 2-5, 2003.

[14] Hrovat, D., Barak, P. and Rabins, M., "Semi-Active versus Passive or Active Tuned Mass Dampers for Structural Control", *Journal of Engineering Mechanics*, Vol. 109, No. 3, pp. 691-705, 1983.

[15] Karnopp, D., "Active and Semi-Active Vibration Isolation", *Journal of Mechanical Design*, Volume 117, pp. 177-186, 1995.

[16] Kareem, A., Kijewski, T., Tamura, Y., Mitigation of Motions of Tall Buildings with Specific Examples of Recent Applications, *Wind and Structures*, Vol 2, n3, pp 201-251, 1999

[17] Rao, S., *Mechanical Vibrations*, Prentice Hall, 2003

[18] Warburton, G., "Optimum absorber parameters for various combinations of response and excitation parameters", *Earthquake Eng. Struct. Dyn.,* 10, pp.381-401, 1982.

[19] Nakanno, K., Suda, Y. and Nakadai, S., "Self-powered active vibration control using a single electric actuator", *Journal of Sound and Vibration*, 260 21-235,2003

[20] Scruggs, J. and Lindner, D., "Active energy control in civil structures", *SPIE Symposium on Smart Structures and Materials*, Newport Beach, CA, 1999.

[21] McCorkle, D., *US Patent*, 5,160,896, 1992

[22] Joseph, L., Poon, D. and Sbieb, S., "Ingredients of high-rise design", technical report, 2006

[23] *Kollmorgen Linear Motors Aim to Cut Cost of Semiconductors and Electronics Manufacture,* Kollmorgen, Radford, VA, U.S.A.,1997.

[24] Honda, J. and Admas, J., "Class D Audio Amplifier Basics," technical paper on International rectifier website, http://www.irf.com/technicalinfo/appnotes.htm.